

# Exploring the Potential of Spiking Neural Networks in UWB Channel Estimation

Youdong Zhang<sup>†</sup>, *Graduate Student Member, IEEE*, Xu He<sup>†</sup>, *Graduate Student Member, IEEE*, Xiaolin Meng<sup>\*</sup>

**Abstract**—Although existing deep learning-based Ultra-Wide Band (UWB) channel estimation methods achieve high accuracy, their computational intensity clashes sharply with the resource constraints of low-cost edge devices. Motivated by this, this letter explores the potential of Spiking Neural Networks (SNNs) for this task and develops a fully unsupervised SNN solution. To enable a comprehensive performance analysis, we devise an extensive set of comparative strategies and evaluate them on a compelling public benchmark. Experimental results show that our unsupervised approach still attains 80% test accuracy, on par with several supervised deep learning-based strategies. Moreover, compared with complex deep learning methods, our SNN implementation is inherently suited to neuromorphic deployment and offers a drastic reduction in model complexity, bringing significant advantages for future neuromorphic practice.

**Index Terms**—SNNs, Unsupervised Learning, Neuromorphic, UWB, Channel Estimation

## I. INTRODUCTION

UWB plays a vital role in Positioning, Navigation and Timing (PNT) tasks, precision agriculture, smart homes, and other domains where GNSS PNT does not function well due to signal obstruction [1]. As a Radio Frequency (RF) technology, assessing the channel state of UWB links is therefore of great importance [2]. For example, in many UWB-based PNT applications, special attention is paid to distinguish Line-Of-Sight (LOS) or Non-Line-Of-Sight (NLOS) channels so that outliers can be filtered out or specifically compensated [3][4].

A large body of work has already embraced learning-based approaches, confirming the value of deep learning techniques for UWB channel estimation [5]. Recent studies have concentrated on algorithmic innovations to further improve estimation accuracy (e.g., [6] and [7]), whilst some researchers have begun exploring large-scale models, achieving noticeable gains [8]. However, these highly complex models incur heavy computational loads, making them ill-suited for the low-cost embedded devices typical of UWB systems. Consequently, researches such as [4] and [9] stress the need for practical, resource-efficient learning-based solutions when deploying UWB channel estimation at the edge.

SNNs, widely regarded as the third generation of neural

This work was supported by the Natural Science Foundation of Jiangsu Province under Grant No. BK20243064. Xu He receives support from the Postgraduate Research & Practice Innovation Program of Jiangsu Province under Grant No. SJCX24\_0067 and SEU Innovation Capability Enhancement Plan for Doctoral Students under Grant No. CXJH\_SEU 24204.

*Xu He & Youdong Zhang contributed equally, so Xu He is the co-first author. Corresponding author: Xiaolin Meng.*

networks, more faithfully reproduce the dynamics of real neural systems than conventional Artificial Neural Networks (ANNs) [10]. Although training SNNs is more challenging than ANNs, their potential for dramatic gains in computational efficiency and ultra-low-power neuromorphic deployment is undoubtedly a major treasure [11]. To our knowledge, virtually no work has explored SNN-based solutions for UWB applications. Only [12] and [13], which address SNN-based classification of Impulse Radio (IR)-UWB radar signals, far away from the standard UWB sensors' channel estimation problem tackled here. This gap motivates our work.

To sidestep the training difficulties commonly associated with SNNs, we adopt the Liquid State Machine (LSM) [14], a recurrent SNN with fixed synaptic weights, to extract spiking representations of both UWB RF channel features and Channel Impulse Response (CIR) features after spike encoding. Specifically, we first engineer the UWB channel data into a form compatible with spike-based representation learning, and then develop a fully unsupervised SNN pipeline (Section II) for channel estimation. Evaluated on the public eWINE benchmark [15], this work achieves performance comparable to that of conventional supervised learning methods. The principal contribution of this letter is thus to demonstrate the viability of SNNs for UWB channel estimation, offering a practical solution and a new reference point for future edge-intelligent mobile applications.

## II. ALGORITHM DESIGN

The proposed fully unsupervised SNN method is illustrated in Figure 1. It consists of two main components: a feature engineering block and a liquid channel state estimation block.

### A. Feature Engineering Block

*RF Feature Processing and Spike Encoding:* The RF chip of the DW1000-based commercial UWB module exposes RF features that can be used to analyze channel state (details can be found in Table I of [1] and its accompanying notes). These features include statistical indicators of ranging observations and noise levels, first path metrics, channel-quality and energy metrics, forming a 10-dimensional feature vector. To make the data compatible with the subsequent SNN, we apply rate encoding [16], a simple yet effective spike encoding method, to

The authors are with the School of Instrument Science and Engineering, the China-UK Research Centre on Intelligent Mobility, State Key Laboratory of Comprehensive PNT Network and Equipment Technology, Southeast University, Nanjing 210096, China (e-mail: xiaolin.meng@seu.edu.cn).

Color versions of one or more of the figures in this article are available online at <http://ieeexplore.ieee.org>

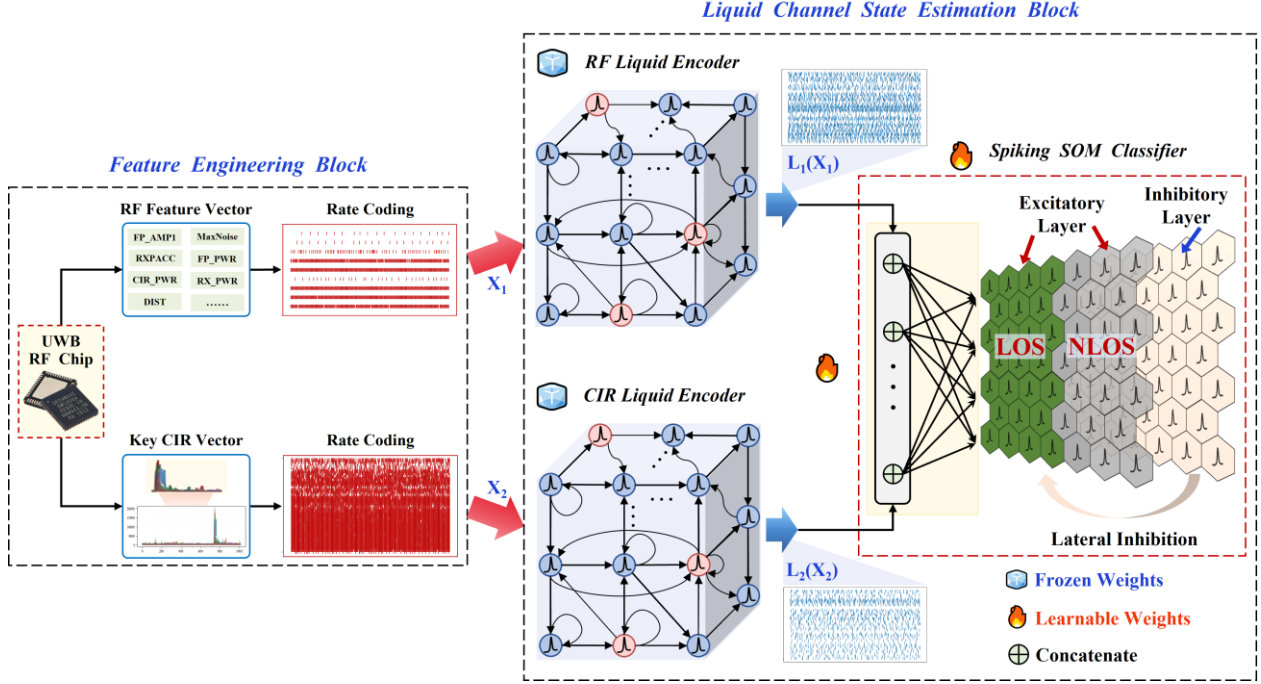


**Fig. 1.** The proposed method.

convert the RF feature vector into a spiking pattern that serves as the input ( $X_1$ ) to the RF liquid encoder.

**CIR Feature Processing and Spike Encoding:** Compared with the RF feature vector, the UWB CIR signal carries richer channel information. The CIR data format supplied by DW1000-based devices depends on the selected Pulse Repetition Frequency (PRF) [4]: at 64 MHz the CIR is delivered as a 1024-sample real sequence, whereas at 16 MHz it is a 992-sample complex sequence. This letter focuses on the real CIR sequence obtained with PRF = 64 MHz.

Earlier work [17] has shown that, for this configuration, the 50 samples starting from FP\_IDX (register index of the first-arrival path peak) are the most discriminative for NLOS identification, a finding subsequently exploited in [4] and [10]. More recent studies [1] and the creators of the eWINE dataset [15] have argued that 120 samples starting from FP\_IDX are beneficial for channel modeling. Therefore, we extract two candidate segments: 50-length and 120-length CIR vectors.

Following the previous demonstration [9] that padding the raw CIR sequence can reduce the representational gap between a 1D discrete vector and the CIR waveform image, we apply uniform padding with a spacing of 10 samples to both extracted segments. The padded vectors are then converted into spike trains via frequency encoding, yielding the input pattern ( $X_2$ ) for the CIR liquid encoder. The same padding and encoding procedures are applied regardless of segment length to ensure consistent experimental conditions.

### B. Liquid Channel State Estimation Block

**Liquid Encoders:** Many deep learning studies rely solely on CIR for UWB channel estimation [6]. Yet, under complicated multipath environments, CIR alone often confuses NLOS with LOS signals. Works like [2] and [4] therefore advocate fusing RF features with CIR for more robust estimation. Accordingly,

we feed the spike-encoded RF and CIR streams into two separate liquid encoders to extract their spiking patterns, denoted  $L_1(X_1)$  and  $L_2(X_2)$  in Figure 1.

As a spiking counterpart to recurrent networks, the liquids in LSM transform input features into high-dimensional spiking representations through a randomly recurrent layer of spiking neurons. Crucially, this mapping is achieved with minimal time cost and no training [14], sidestepping the design and training hurdles of elaborate SNNs.

Both the RF and CIR liquid encoders are built with Leaky Integrate-and-Fire (LIF) neurons [11]. The RF and CIR liquid encoders contain 400 and 500 LIF neurons, respectively. Each liquid encoder comprises excitatory and inhibitory neurons (color-coded in Figure 1). Synapses are randomly initialized, sparse, and include a fraction of self-connections.

Since we operate under discrete time steps, the discretized LIF neurodynamics can be described as follows:

$$V[t] = V[t-1] - \frac{1}{\tau_m} (V[t-1] - V_{rest}) + WX[t] - S[t]\theta \quad (1)$$

Where,  $V[t]$  is the membrane potential,  $\tau_m$  is the membrane time constant,  $V_{rest}$  is the resting potential,  $W$  are the synaptic weights,  $X[t]$  is the input and  $\theta$  is the threshold. Note that if a neuron is fired at time  $t$ , its membrane potential is reset at that moment. Therefore, the membrane voltage at time  $t$  consists of the decay term  $(V[t-1] - V_{rest})/\tau_m$ , the input term  $WX[t]$ , and the reset term  $S[t]\theta$ . The spiking activation function  $S[t]$  is defined in (2) as follows:

$$S[t] = \begin{cases} 1, & \text{if } V[t] \geq \theta \\ 0, & \text{otherwise} \end{cases} \quad (2)$$

The related LIF parameters follow [19]. Compared with many deep learning models that rely on large Convolutional Neural Networks (CNNs) or attention mechanisms (e.g., [6] and [8]), the liquid encoders offer markedly lower computational cost and higher efficiency.

> REPLACE THIS LINE WITH YOUR MANUSCRIPT ID NUMBER (DOUBLE-CLICK HERE TO EDIT) <

*Spiking SOM Classifier:* Since [4] has already discussed the benefits of mapping RF and CIR features through separate branches, we omit that discussion here. After the two liquid encoders produce their respective spike patterns, the resulting 1D tensors are concatenated into a joint spike pattern that serves as input to the spiking Self-Organizing Map (SOM) classifier [18], a spike-based variant of the SOM. The spiking SOM is likewise implemented with LIF neurons.

Unlike traditional SOM, competition is decided by counting input spikes: the neuron receiving the largest number of spikes is declared the winner. The winner then strengthens the activation of its neighbors, which learn similar spike patterns under the same input, while simultaneously exerting lateral inhibition on non-neighboring neurons, reducing their probability of firing. Classification is performed by choosing the label whose associated neurons exhibit the highest average spike count per sample. Due to space limitations, more details on the spiking SOM see [18].

### III. EXPERIMENT AND ANALYSIS

We evaluate our method on the publicly available eWINE benchmark [15]. All LIF neurons are simulated with the open-source library BindsNET [19], of which the first author is a contributing developer. Experiments were run on a workstation with 32 CPU cores, 251 GB RAM, and an RTX 3090 GPU. The liquid encoders use fixed, untrained weights; only the spiking SOM is trained, using the unsupervised, biologically inspired Spike Timing Dependent Plasticity (STDP) rule [20]. The dataset is split 5:2 into training and test sets, with no overlap.

In the spirit of exploring the value and potential of SNNs for UWB channel estimation, this letter designs a variety of strategies for benchmarking. Moreover, we also compare performance across 50- and 120-sample truncations. In addition, we benchmark our approach against several recent deep learning solutions.

All strategies are defined as follows, please refer to Table I for a more clearly understanding.

□ *Strategy1:* The 50-sample CIR segment is spike-encoded into  $X_2$  and fed to the CIR liquid encoder to produce spike pattern  $L_2(X_2)$ . Following the pipeline in Figure 1,  $L_2(X_2)$  is fused with the RF-branch spike pattern  $L_1(X_1)$  and classified by the spiking SOM.  
□ *Strategy2:* Same as Strategy1, but uses a 120-sample CIR

segment.

- *Strategy3:* Same as Strategy1, but ablating CIR features' contribution entirely.
- *Strategy4:* Same as Strategy3, but ablating the RF liquid encoder.
- *Strategy5:* Same as Strategy1, but ablating RF features' contribution entirely.
- *Strategy6:* Same as Strategy5, but ablating the CIR liquid encoder.
- *Strategy7:* Same as Strategy2, but ablating RF features' contribution entirely.
- *Strategy8:* Same as Strategy7, but ablating the CIR liquid encoder.
- *Strategy9:* Same as Strategy1, but ablating all liquid encoders.
- *Strategy10:* Same as Strategy2, but ablating all liquid encoders.

The evaluation metrics of all strategies are quantified in Table I. The results demonstrate that the proposed Strategy1 and Strategy2 outperform all other methods. In fact, every other entry in Table I can be considered an ablation study of these two strategies. The choice between 50 and 120 CIR samples has only a minor impact on accuracy, but the longer segment (Strategy2) is slightly weaker.

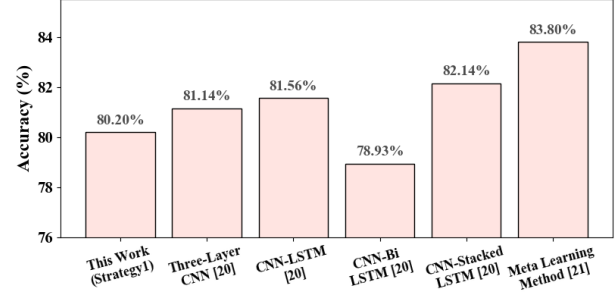


Fig. 2. Comparison of this work and deep learning baselines.

Introducing the liquid encoder is beneficial. The clearest evidence is seen when Strategy9 and Strategy10 ablate all liquid encoders, compared with Strategy1 and Strategy2, all performance metrics plummet by nearly 30%. Moreover, removing the CIR liquid encoder from Strategy7 to obtain Strategy8 causes a drop of roughly 10 percentage points across all metrics. A similar trend is observed when comparing Strategy5 and Strategy6, as well as Strategy3 and Strategy4.

TABLE I  
EVALUATIONS OF ALL DESIGNED STRATEGIES ON THE EWINE BENCHMARK

	Model Structures				Metrics			
	Feature Engineering	RF Liquid Encoder	CIR Liquid Encoder	Spiking SOM Classifier	Accuracy	Precision	Recall	F1 Score
<b>Strategy1</b>	<b>RF+CIR(50)</b>	√	√	√	<b>80.2%</b>	<b>76.3%</b>	<b>87.3%</b>	<b>81.4%</b>
<b>Strategy2</b>	<b>RF+CIR(120)</b>	√	√	√	<b>80.0%</b>	<b>82.5%</b>	<b>75.7%</b>	<b>79.0%</b>
Strategy3	RF	√	✗	√	77.0%	81.8%	69.1%	74.9%
Strategy4	RF	✗	✗	√	51.3%	51.1%	46.3%	48.6%
Strategy5	CIR(50)	✗	√	√	58.1%	57.3%	61.4%	59.3%
Strategy6	CIR(50)	✗	✗	√	50.1%	49.8%	53.7%	51.7%
Strategy7	CIR(120)	✗	√	√	60.3%	58.9%	66.9%	62.6%
Strategy8	CIR(120)	✗	✗	√	49.9%	49.6%	48.2%	48.9%
Strategy9	RF+CIR(50)	✗	✗	√	51.2%	50.9%	53.0%	51.9%
Strategy10	RF+CIR(120)	✗	✗	√	49.6%	49.3%	50.8%	50.0%

> REPLACE THIS LINE WITH YOUR MANUSCRIPT ID NUMBER (DOUBLE-CLICK HERE TO EDIT) <

Additionally, this letter also includes several recent supervised deep learning baselines for comparison. For instance, [21] reports multiple baseline results on the eWINE dataset, including classic multi-layer CNNs and CNN-LSTM models with different Long Short-Term Memory (LSTM) architectures. [22] presents a meta learning-based channel estimation strategy. Figure 2 records the comparison of this work (Strategy1) with involved baselines. Due to space constraints, the parameter details of all baselines are omitted here; please refer to their original works [21][22]. The results show that our fully unsupervised SNN scheme achieves accuracy close to that of traditional supervised deep learning methods. However, in contrast to deep learning models, our method offers unique advantages in computational efficiency and neuromorphic deployment compatibility. These attributes are supported by [23], which confirms the low power consumption and real-time processing capabilities of LSM.

*Note.* Data and core code can be available from the authors upon reasonable request.

#### IV. DISCUSSION AND CONCLUSION

This letter explores the potential of SNNs for UWB channel estimation, proposing a fully unsupervised SNN approach that achieves accuracy comparable to conventional deep learning methods on the public benchmark. The design deliberately adheres to unsupervised principles: the LSM encoder requires no training. Although the spiking SOM classifier is trained with STDP, its simplicity is far more efficient than end-to-end training of a complex SNN. The structure of liquid encoders and readout classifier could be further optimized. Moreover, while training a large end-to-end SNN from scratch remains difficult, lightweight ANN-to-SNN conversion via frameworks such as SpikingJelly [24] is worth investigating. Finally, we encourage the community to explore the neuromorphic deployment potential of both this work and future ANN2SNN schemes, enabling stronger computational efficiency and lower power consumption for edge-intelligent mobile applications.

#### REFERENCES

- [1] M. Wang et al., "A 600-M UWB Ranging Dataset With Radio Frequency Features and Deep Learning Applications," *IEEE Sensors Journal*, vol. 25, no. 21, pp. 39901-39914, Nov, 2025.
- [2] Y. Wu, et al., "Self-Attention-Assisted TinyML With Effective Representation for UWB NLOS Identification," *IEEE Internet of Things Journal*, vol. 11, no. 15, pp. 25471-25480, Aug, 2024.
- [3] D. Kim, et al., "UWB Positioning System Based on LSTM Classification With Mitigated NLOS Effects," *IEEE Internet of Things Journal*, vol. 10, no. 2, pp. 1822-1835, 15 Jan, 2023.
- [4] X. He, et al., "Enhance UWB Performance Using Dynamic AI-Enabled Approach," *IEEE Internet of Things Journal*, 2025.
- [5] F. Che, et al., "Feature-Based Generalized Gaussian Distribution Method for NLoS Detection in Ultra-Wideband (UWB) Indoor Positioning System," *IEEE Sensors Journal*, vol. 22, no. 19, pp. 18726-18739, Oct. 2022.
- [6] Y. Pei, et al. "FCN-Attention: A Deep Learning UWB NLOS Classification Algorithm Using Fully Convolution Neural Network With Self-Attention Mechanism," *Geo-spatial Information Science*, vol. 27, no. 4, pp. 1162-1181, Mar, 2023.
- [7] B. Deng, et al., "UWB NLOS Identification and Mitigation Based on Gramian Angular Field and Parallel Deep Learning Model," *IEEE Sensors Journal*, vol. 23, no. 22, pp. 28513-28525, Nov. 2023.
- [8] H. Yang et al., "Fuzzy Transformer Machine Learning for UWB NLOS Identification and Ranging Mitigation," *IEEE Transactions on Instrumentation and Measurement*, vol. 74, pp. 1-17, 2025, Art no. 8503817.
- [9] X. He, et al., "A Lightweight UWB NLOS Detection Algorithm Using Referenced CIR Similarity Metrics," *IEEE Wireless Communications Letters*, vol. 13, no. 10, pp. 2797-2801, Oct. 2024.
- [10] W. Maass, "Networks of Spiking Neurons: The Third Generation of Neural Network Models," *Neural Networks*, vol. 10, no. 9, pp. 1659-1671, Dec. 1997.
- [11] K. Roy, et al., "Towards Spike-Based Machine Intelligence With Neuromorphic Computing," *Nature*, vol. 575, no. 7784, pp. 607-617, Nov. 2019.
- [12] S. Wang et al., "Hand Gesture Recognition Using IR-UWB Radar With Spiking Neural Networks," *IEEE International Conference on Artificial Intelligence Circuits and Systems (AICAS)*, 2022, pp. 423-426.
- [13] M. O'halloran, et al., "Spiking Neural Networks for Breast Cancer Classification in a Dielectrically Heterogeneous Breast," *Progress in Electromagnetics Research-PIER*, vol. 113, pp. 413-428, 2011.
- [14] W. Maass, et al., "Real-Time Computing Without Stable States: A New Framework for Neural Computation Based on Perturbations," *Neural Computation*, vol. 14, no. 11, pp. 2531-2560, Nov. 2002.
- [15] K. Bregar, et al., "Improving Indoor Localization Using Convolutional Neural Networks on Computationally Restricted Devices," *IEEE Access*, vol. 6, pp. 17429-17441, Mar. 2018.
- [16] R. Rullen, et al., "Rate Coding Versus Temporal Order Coding: What the Retinal Ganglion Cells Tell the Visual Cortex," *Neural Computation*, vol. 13, no. 6, pp. 1255-1283, Jun. 2001.
- [17] S. Kram, et al., "UWB Channel Impulse Responses for Positioning in Complex Environments: A Detailed Feature Analysis," *Sensors*, vol. 19, no. 24, p. 5547, Dec. 2019.
- [18] H. Hazan, et al. "Unsupervised Learning With Self-Organizing Spiking Neural Networks," *International Joint Conference on Neural Networks (IJCNN)*, IEEE, 2018.
- [19] H. Hazan, et al. "BindsNET: A Machine Learning-Oriented Spiking Neural Networks Library in Python," *Frontiers in Neuroinformatics*, vol. 12, p. 89, Dec. 2018.
- [20] Harel. Shouval, et al. "Spike Timing Dependent Plasticity: A Consequence of More Fundamental Learning Rules," *Frontiers in Computational Neuroscience*, vol. 4, p. 19, Jul. 2010.
- [21] J. Jiang, et al., "UWB NLOS Classification Using Deep Learning Method," *IEEE Communications Letters*, vol. 24, no. 10, pp. 2226-2230, Oct. 2020.
- [22] Y. Liu, et al., "Hard Sample Meta-Learning for CIR NLOS Identification in UWB Positioning," *IEEE Internet of Things Journal*, vol. 12, no. 10, pp. 14136-14149, May. 2025.
- [23] C. Shi et al., "Ghost Reservoir: A Memory-Efficient Low-Power and Real-Time Neuromorphic Processor of Liquid State Machine With On-Chip Learning," *IEEE Transactions on Circuits and Systems II: Express Briefs*, vol. 71, no. 10, pp. 4526-4530, Oct. 2024
- [24] W. Fang et al., "SpikingJelly: An Open-Source Machine Learning Infrastructure Platform for Spike-Based Intelligence," *Science Advances*, vol. 9, no. 40, p. eadi1480, Oct. 2023.